Spring 2017

Optimization of Lateral Jets for Guiding Supersonic Missiles

Anne M. Pirie
amp179@zips.uakron.edu

Samuel J. Rhoades
sjr59@zips.uakron.edu

Emily C. Slovan
ecs47@zips.uakron.edu

Senior Design Final Report:

Optimization of Lateral Jets for Guiding Supersonic Missiles

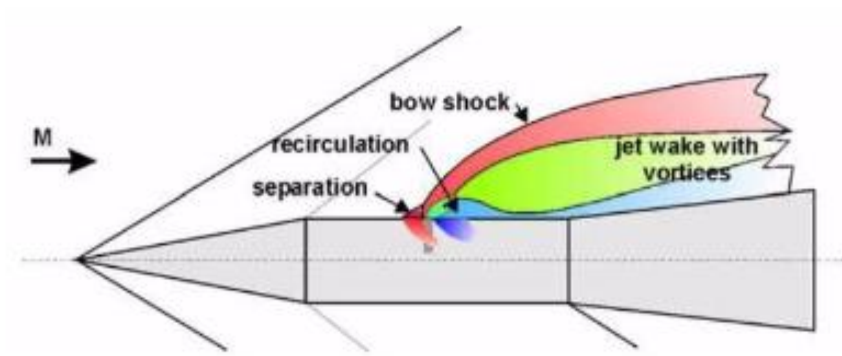

Faculty Advisor: Dr. Alex Povitsky

Honors Student(s): Anne Pirie

NonHonors Student(s): Emily Slovan, Samuel Rhoades

Abstract:

This project seeks to improve the guidance of supersonic missiles with lateral jets. This is achieved by quantifying and optimizing the pressure distributions created along the surface of the missile by the jets in different configurations. *The jets themselves must be considered as well as turbulent and compressible effects and thermal losses.* To explore these effects, flat plate geometry experiments of high-speed jet in cross-flow are considered for validation purpose. Group members are using FLUENT to reproduce experimental results of a jet in crossflow attempting to achieve higher accuracy by use of various solution methods. Two and three dimensional models of air vehicles equipped with jet control created using Creo and corresponding flow simulations generated in Ansys FLUENT.

Acknowledgements: Problem initiated by Eglin Airforce Base Research Laboratory (Dr. D. Reasor) where Dr. Povitsky was a summer faculty fellow in 2016. Special thanks to graduate students Kristopher Pierson and Himel Barua.

TABLE OF CONTENTS

Introduction

The goal of our Senior Design project is to optimize the use of lateral jets as a guidance mechanism for supersonic missiles. Previous work done on this project by Kristopher Pierson and Dr. Alex Povitsky and summarized in their paper, "Modeling of lateral jets for guidance of supersonic missiles" [1] sought to reproduce the experimental observations made [3] of a jet in crossflow across a flat plate using OpenFOAM software. Since all the software packages relevant to this project were new to our group members, we have tried to limit ourselves to the use of Ansys Fluent. Using his flow simulations as a reference, we are worked to ensure these same results in Fluent. In these models we hoped to observe broadly the development of the boundary layer along the flat plate surface, the separation zone at the jet inlet, a recirculation zone caused after the jet disturbance and the shockwaves downstream from the jet.

More specifically, though, we would like to quantify pressure distribution along the surface of a body caused by a lateral jet. In order to be able to model the scenarios more relevant to our research we have begun to use more complex geometries that incorporate the curved nose cones and fins observed in missile profiles. Beginning with two-dimensional axisymmetric scenarios so as to determine the correct boundary conditions (or ranges of boundary conditions) we have carried these over to three dimensional studies with mapped meshing to allow us to closely observe the effects of jets and fins on the flow development and pressure distribution.

The Fluent simulation allows each of the complex geometries' flow to be evaluated based on the continuity equation, energy equation and the Navier-Stokes equation. For turbulent flow the Reynolds Averaged versions of these are used as described by Confluence Cornell [6]. The figure below shows the relevant forms of these equations as well as the Spalart-Allmaras model described after. The Spalart-Almaras model for viscosity was chosen for our simulations due, in part, to its likelihood to lend stability to the system and drive it towards convergence. It was developed to solve for kinematic eddy viscosity. Fluent solves for this along with velocity (in the x,y, and z directions), pressure, and temperature.

$$\frac{\partial \rho}{\partial t} + \frac{\partial}{\partial x_i}(\rho u_i) = 0 \qquad (1)$$

$$\rho(\frac{\partial U_i}{\partial t} + \frac{\partial}{\partial x_j}(U_i U_j)) = -\frac{\partial P}{\partial x_i} + \frac{\partial}{\partial x_j}(2\mu S_{ij} - \rho\overline{u_i' u_j'}) \qquad (2)$$

$$\frac{\partial}{\partial t}(\rho e_0) + \frac{\partial}{\partial x_j}[\rho u_j e_0 + u_j p + q_j - u_i \tau_{ij}] = 0 \qquad (3)$$

$$-\overline{u_i' u_j'} = 2\nu_T S_{ij} \qquad (4)$$

The Continuity Equation is given by equation 1

The Reynolds Averaged Navier-Stokes equation is given by equation 2

The conservation of energy equation is given by equation 3

The Spalart-Allmaras turbulence model is given by equation 4

Figure 1: Fluent background equations as presented by Confluence Cornell

I. 3-Dimensional Jet in Cross Flow Analysis

Table 1

FLUENT Settings	
Solver and Models	
Solver	Density-Based
Viscous Model	Turbulent, K-Epsilon
Density	Ideal Gas (Air)
Energy Equation	On
Solution Methods	
Pressure-Velocity Coupling	Coupled
Density, Momentum, Energy	Second Order Upwind

We were to start out analysis on a 3 dimensional flat plate geometry that was parallel to previous experiments run. (1) For the analysis we ran two different sets of tests - a coarse grid and a more refined grid. Initially we ran the coarse grid because of license restrictions that held us to a maximum of 512,000 elements per solution run. We later had the capability of running a solution with element restriction of greater than one million. For both the coarse and fine grid we had the same boundary conditions. Crossflow inlet had a velocity of 448m/s (Ma = 1.6), and Jet inlet had a velocity of 314.8m/s (Ma = 1.0).

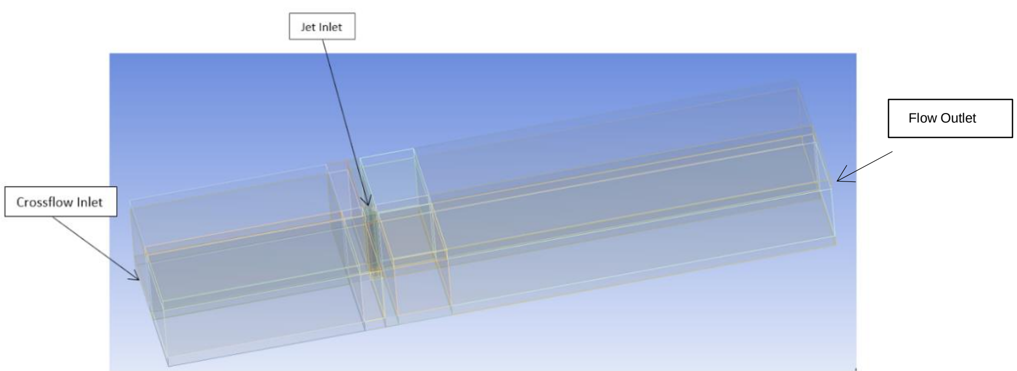

Figure 2: Flat Plate Analysis Setup Schematic

The boundary conditions for the top, bottom and side walls were all to be considered as walls. Jet inlet and crossflow inlet were both set as velocity inlets and the outlet was set to a pressure outlet.

With the boundary conditions in place, we were to recreate a previous experiment (1) that was run and described in a research paper written by graduate student Kristopher Pierson. There were results we would like to be able to compare our solution to in order to move forward with the project. Before we move on to the main part of the project we would like to make sure we have a converging solution with the given jet geometry. During our research we also ran different geometries to explore a possibly better option for our optimization. In order for our solution to converge the magnitudes of the residuals were to drop below 1e-3.

A. 3-Dimensional Jet-in Crossflow Analysis (Coarse Grid)

For the 3D flat plate with a coarse grid we had the dimensions of 76m width, 36m height and a 205.5m length. We had the shortened length for the coarser grid to make up for the amount of cells that we would need to lose in order to fall within the bounds of the license restriction in FLUENT. With the max element size of 512,000 elements we were able to create a grid with 510,160 cells. From the beginning we were running a solution with laminar flow and constant density. However, since then we have adjusted to turbulent flow and an ideal gas as the working fluid. When we ran the coarser grid we were unable to achieve the convergence we had hoped to see. There is the start of a solid shock wave near the jet inlet and the start of a reflection and a small recirculation zone just downstream of the jet as shown in figure 1.

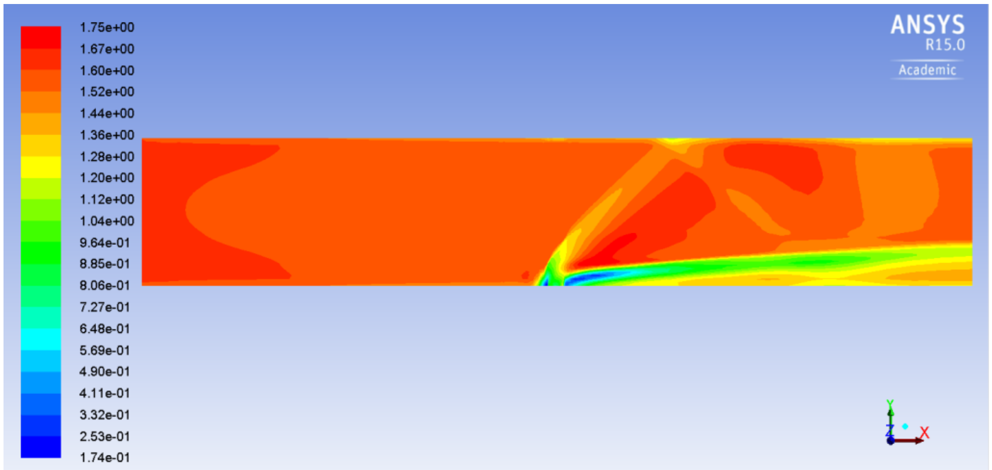

Figure 3: Contours of Mach Number, 3-D Flat Plate, Coarse Grid

There are some concerns when working with so few cells in such a large domain. For this reason we changed the size to a shorter domain to make up for the amount of cells that would need to be cut out. However, even with the flat plate being cut down by 100m the change in cell size was still a big factor for why the solution did not converge. In figure 2 when examined closely there is an apparent change in cell size which affects how the vectors are directed. The cells near the bottom edge of the flat plate need to be more refined in order for the domain to capture the affects the jet is having on the crossflow. There is also an issue when a change in cell size (small cells to large cells) is too drastic which is another issue clearly shown in figure 2.

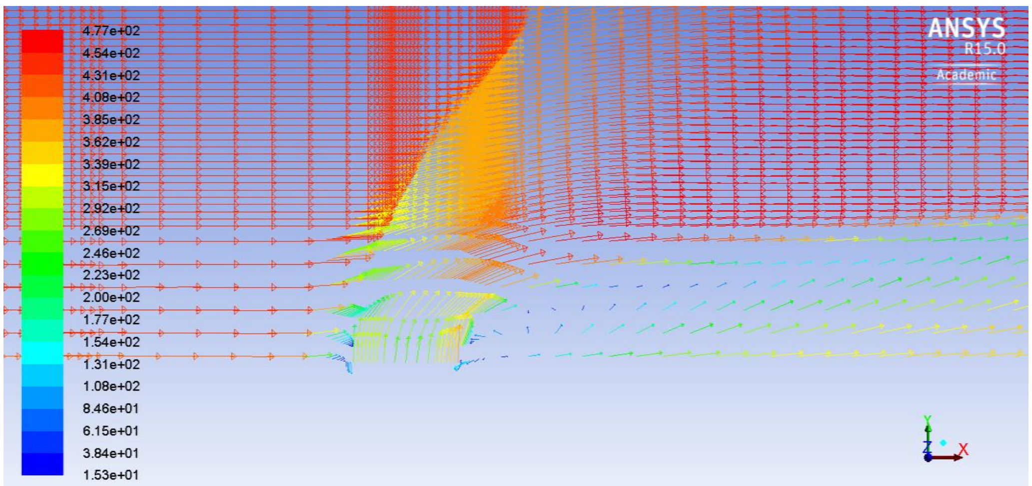

Figure 4: Velocity Vectors, 3-D Flat Plate, Coarse Grid

B. 3-Dimensional Flat Plate Analysis (Fine Grid)

For the finer mesh on the 3D flat plate we were able to create a geometry that had 1.3 million cells. Having the capability to have a mesh so fine opens up the ability to have the longer downstream region. This will in turn benefit the meshing by us being able to have a longer transition period that we were unable to have in the coarser grid. With this grid we also have a closer comparison to the results run experimentally which is what we originally were aiming to accomplish with the flat plate analysis.

During the meshing of the flat plate we were careful not to have a large growth rate in the mesh sections. Having the mesh be separated into many parts along the flat plate we were able to have a very fine mesh close to the bottom of the plate where we should see our boundary layer and pressure distributions. From figure 3 we can see the smooth grid transition from the bottom of the flat plate to the middle section of the flat plate. Now with this mesh we are able to start the comparison to the experiment.

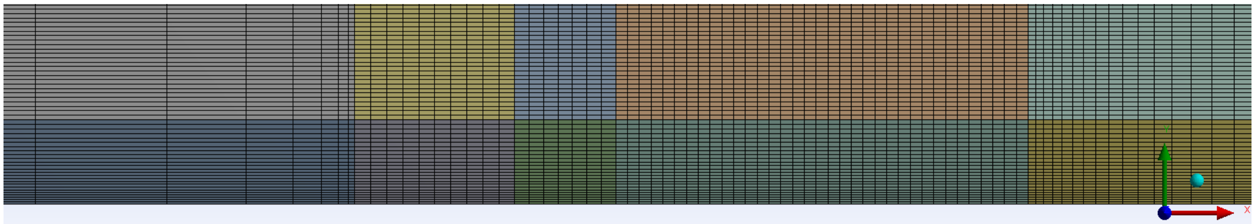

Figure 5: 3-D Flat Plate, Fine Grid

First, the figure 4 shows the pressure distribution computed by the software FLUENT. There are no experimental distributions for the pressure in the report we compared to so the interesting comparisons will follow.

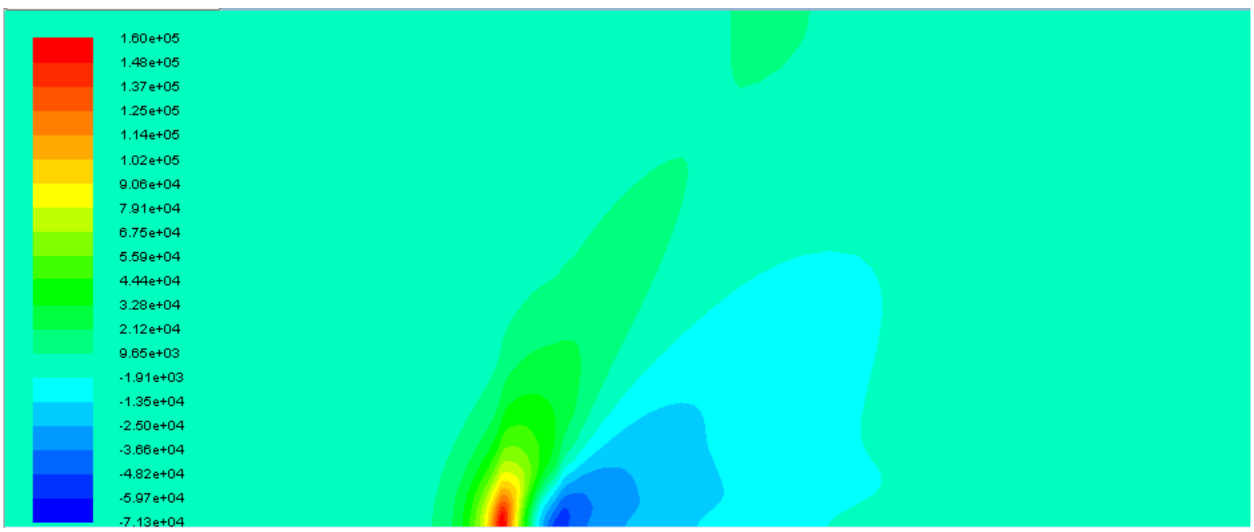

Figure 6: Pressure Distribution, 3-D Flat Plate, Fine Grid

For the velocity vectors we looked to see how the direction is changed before and after where our jet is located. We have a fairly close comparison between the two. We can see in our FLUENT solution where the recirculation section is that parallels that of the experiment. The FLUENT analysis run by our group is figure 5 and the experiment is figure 6.

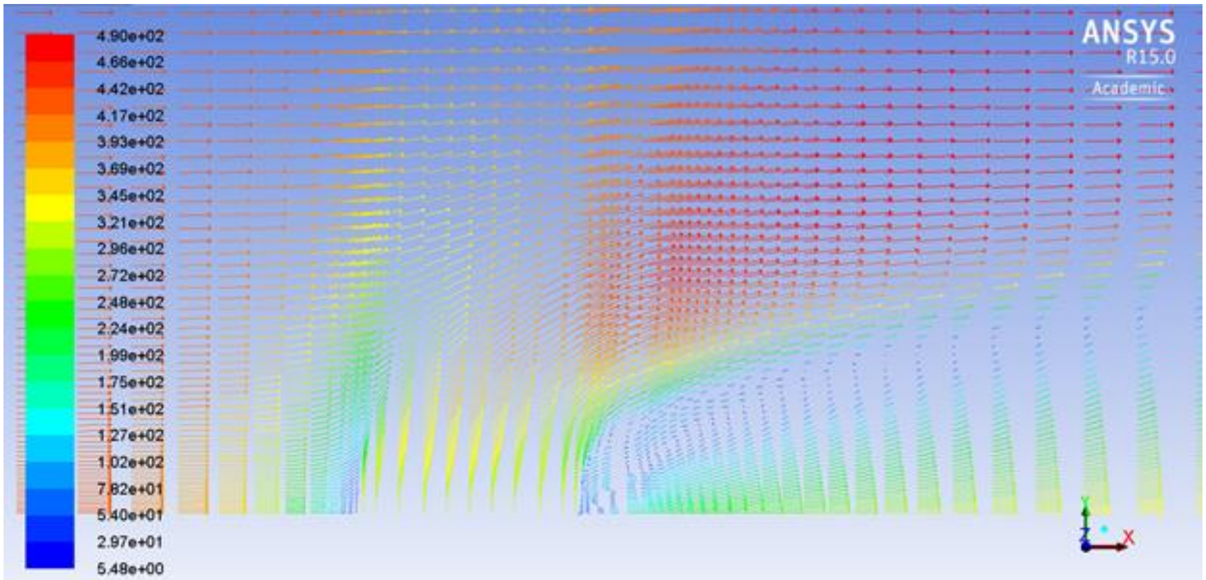

Figure 7: Velocity Vectors, 3-D Flat Plate, Fine Grid

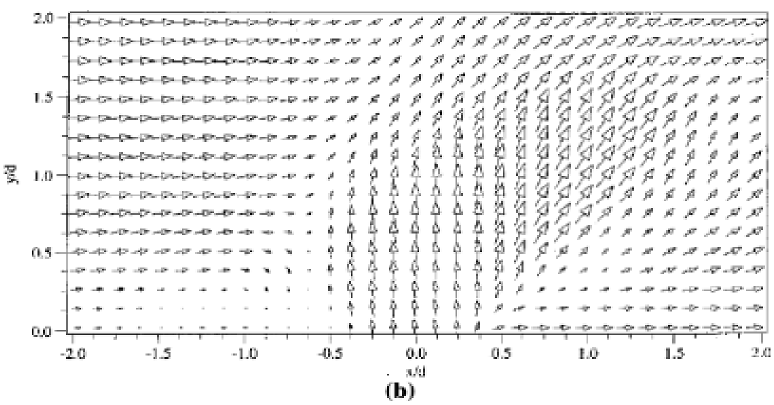

Figure 8: Experimental Velocity vectors

As far as the density comparison between the experiment and our analysis goes we see some good comparisons to make. There is a clear bow shock showing in our FLUENT that is similar to the experimental figure shown. There is also a start to a reflection of the shock wave in FLUENT however not fully developed.

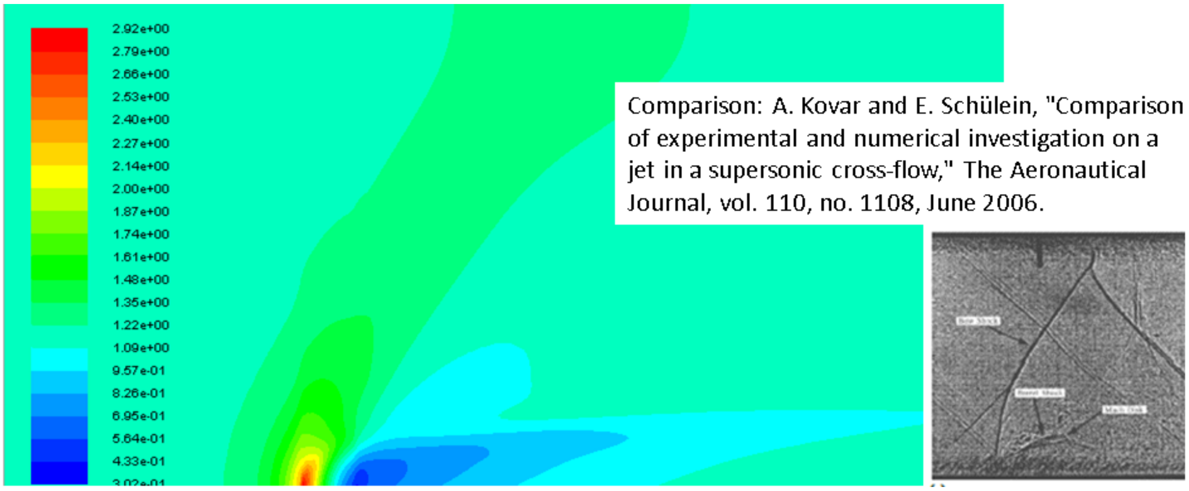

Figure 9: Comparison of Simulated and Experimental changes in Density, 3-D Flat Plate, Fine Grid

For the overall 3D flat plate analysis we were able to achieve our goal of a converging solution. There is an obvious parallel between mesh size and similarities to the experimental results. With the more refined mesh all of the results showed a much closer relationship between each other.

C. 3-Dimensional Jet-in Crossflow Analysis (Elliptical Jet)

We were to also try different jet geometries to analyze the effects it would have on flow downstream. For ours we attempted the use of an elliptical jet in the crossflow. Using all the same boundary conditions and keeping the same area to have the same mass flow rate. The geometry we chose to go with was a 2:1 ratio ellipse seen in the figure below.

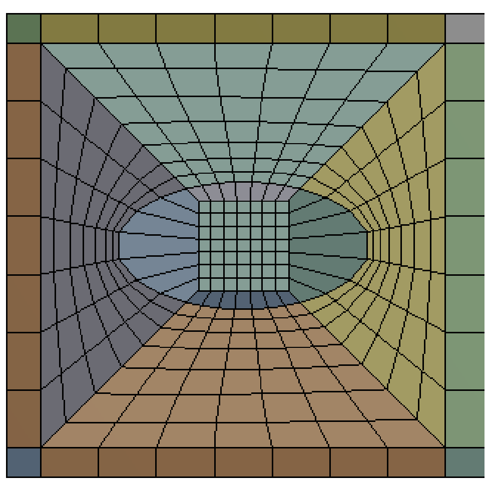

Figure 10

The figures below highlight how the contours of pressure and velocity were solved. The solution began to have a good reflection of a shockwave however it was never fully converged.

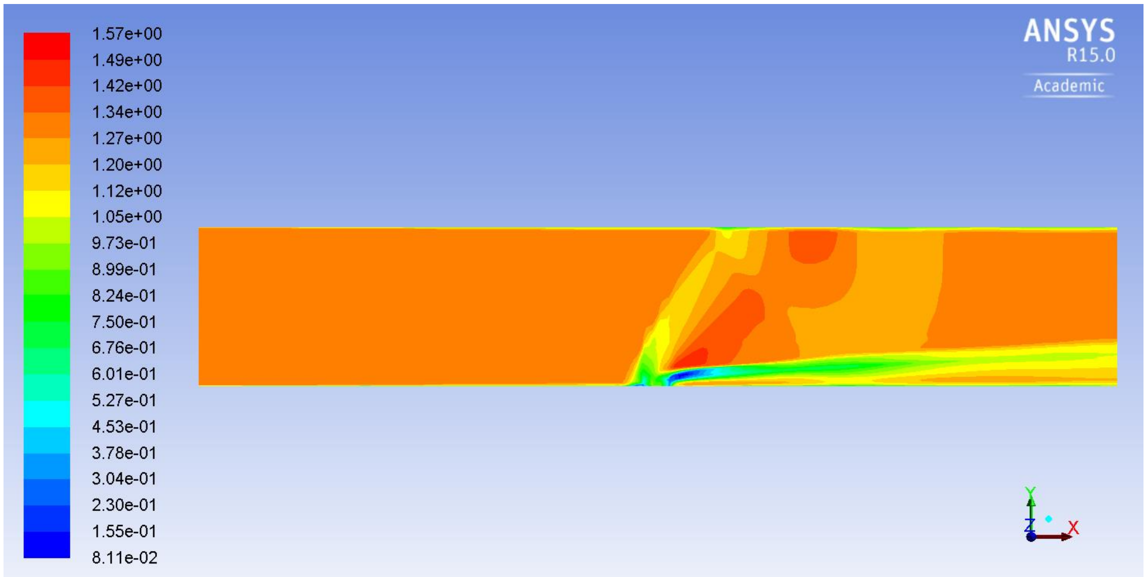

Figure 11 Mach Number Contours

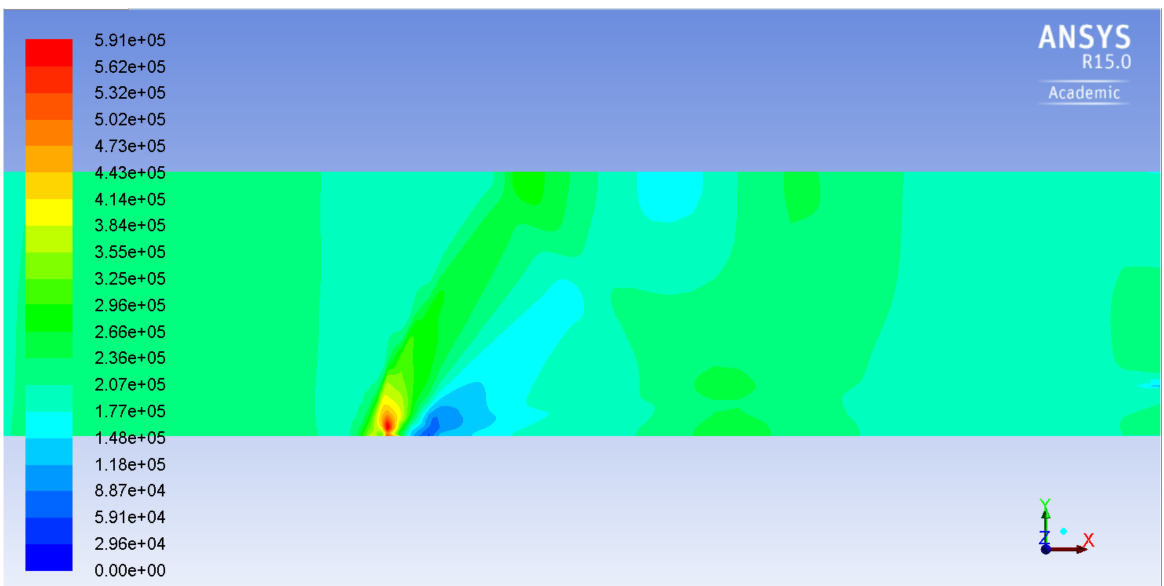

Figure 12 Pressure Contours

II. 2-Dimensional Missile

In the optimization of lateral jets in crossflow to guide supersonic missiles, an essential analysis of a 2D missile was one of the first simulations conducted to gain a better understanding of boundary conditions within the system. In studying the boundary conditions, pressure, velocity and density distributions from the 2D case study, it yielded a strong understanding of the systems response within a free stream fluid system and contributes to a smooth testing for a 3D case study later in the project. There were many case studies conducted by the US military and government research facilities that were referenced in the 2D modeling phase. A case study by Julius Brandeis and Jacob Gill was conducted to study the different missile formations and their interaction with supersonic jets. Through flight, shockwaves are formed due to the sound waves inability to travel upstream and there is a pressure that builds up within the region. The pressure that is produced from the shock wave formed is located at the nozzle of the supersonic jet that is obstructing flow. Further downstream, the pressure reduces and there is an area of separation that is created before the supersonic jet with the separation shock and high surface pressure. It was found that higher Mach numbers between 4.5 and 10 resulted in larger amplification factors that had 0 angle of attack. High force amplification allows for a more controlled force with a supersonic jet thrust. In cases with a lower Mach number, 2, the results showed that there was a substantial loss in the control force amplification with a 0 angle of attack in comparison to cases with a higher Mach number. In the case study conducted by Brandeis and Gill, there were five different missile body designs implemented in the experiment, as seen in Figure 8.

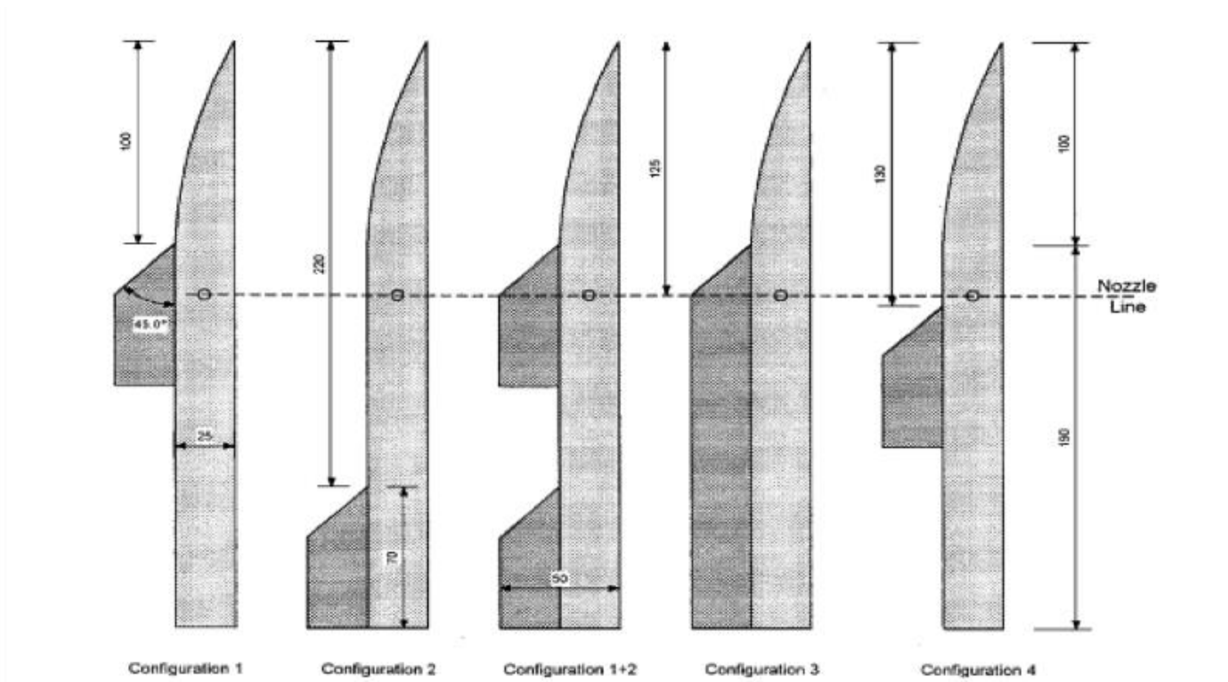

Figure 13: Various fin configurations developed by Brandeiss

A. Geometry

The missile body design remained the same regarding the nose cone and the remaining body; however the fins located on the body varied in size, length and projection from the missile body. The second configuration from Figure 1 is the missile configuration that was implemented in the 2D case study for this senior design project. The design was imported from an external geometry file and modeled with an outer c domain that would later be defined as a free stream surface boundary condition in the 3D case. Once the c domain and missile configuration were modeled within the software, the missile could now be called out as a wall within the modeled system, and the mesh was built in the domain.

B. Mesh

Mesh refinement is a critical step in studying the solution near the wall of the missile. As seen in Figure 13 and 14 below, there is an initial mesh generated on the outer region of the c domain. Staying within the software limits of Fluent, 512,000 elements are able to be created and investigated using mapped faced meshing, edge sizing and bias factor techniques in order to get a more refined mesh moving towards the missile body in the domain. Once the mesh is successfully generated for analysis, boundary conditions can be developed from different named selections within the 2D model. The inlet, outlet and missile are respectively defined within the meshing, and in Fluent they will be titled for their respective boundary conditions in the 2D case. The inlet is defined as a velocity inlet, the outlet is defined as a pressure outlet and the missile body is defined as a wall.

C. Setup and Solution

The next phase in studying the 2D missile case is to properly run the mesh and to get a converged solution that can compute data, and display the shock wave/s formed in the system. From the solution, the contours for velocity, pressure, density and Mach number are shown in figures 4-7 below with the Courant numbers respectively at 200 and 0.9. The Courant number is varied in the solution computations in order to achieve stability and yield a converged solution. Higher Courant numbers are used based on the complexity of the case study, and when first running the computation a lower Courant number was used based on the solution being nonlinear. The pressure region seen in figure X below shows the pressure distribution. Interpreting these results allows us to create a 3D case study analysis that will allow for a more uniform meshing refinement in all coordinate systems, a freestream boundary layer defined by the c domain, and will be encapsulated within the freestream domain large enough to accurately show the new shock wave formed.

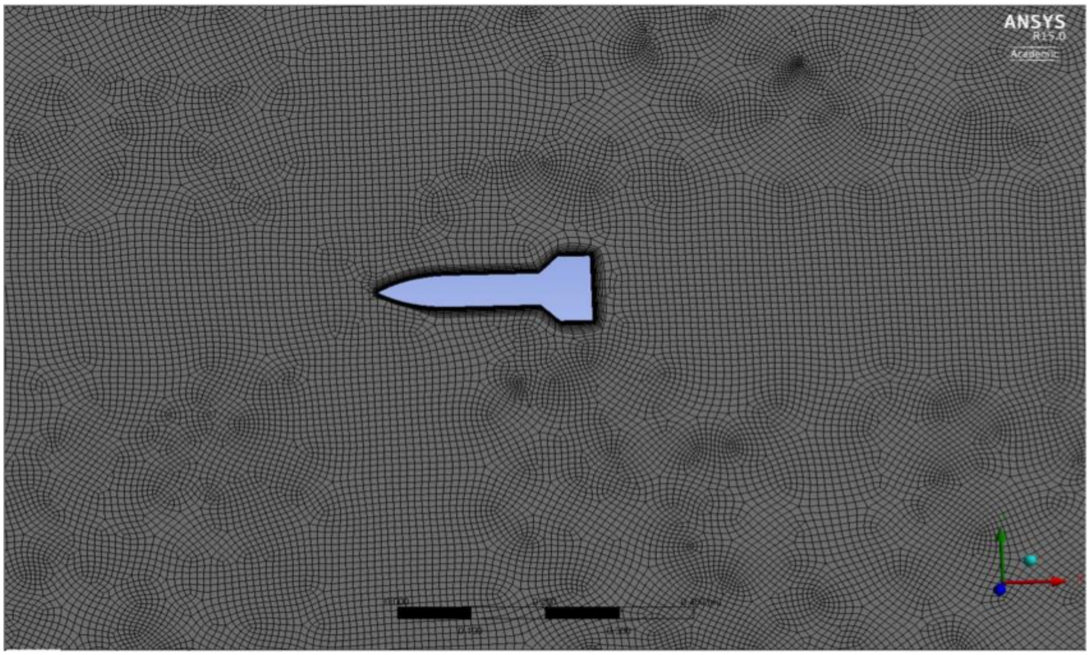

Figure 14: 2D Missile Mesh, Overall Sizing

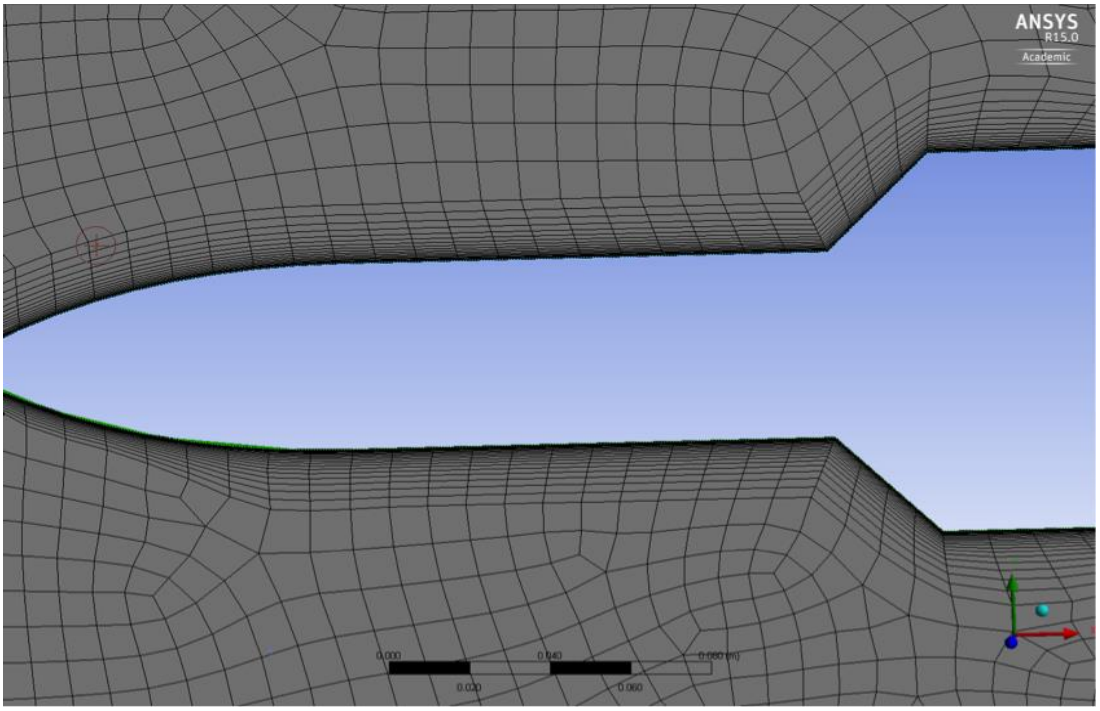

Figure 15: 2D Axisymmetric Missile Mesh, Inflation Layer

III. 3-Dimensional Missile

A. Geometry

Having learned from the two-dimensional geometry building and defining of boundary conditions, we went on to analyze the case of a three-dimensional model. Once again, the missile body dimensions were taken from the configuration 2 shown in figure **1**. This was modeled as a revolve in Creo Parametric and imported into Workbench DesignModeler for use.

The second step was to choose an appropriate fluid domain. The overall C shape used is a common feature of fluid analysis. The dimensions were chosen at various multiples of the chord length of the missile body. The goal in choosing dimensions was, first, to have a domain large enough that lack of computational area for significant features or areas of the flow did not introduce infidelities to the simulated flow with respect to real physical circumstances. Secondly, for the sake of efficiency, it was important not to create a fluid domain that was much larger than necessary. This would both slow down each iteration so that runs could take several hours more than they already did and limit the computers which could be used for the analysis at all. As we considered different domain sizes it was determined that a domain about ten times the chord length was still not large enough to capture the flow accurately. At a radius of fifteen times the chord length we saw developed shockwaves whose furthest bounds were within this domain (as will be explored later). For this reason we did not further pursue obtaining a solution in the fluid domain with a radius of twenty times the chord length that we prepared. It is possible, however, that this would be necessary for different Mach numbers and/or angles of attack.

After some work with the mesh described in the next section, it proved to be necessary to further divide the geometry so that locations of greater interest could be analyzed more effectively. To do this we created a cylinder approximately five times the diameter of the missile that extended about a quarter of the missile chord length in front and behind it. This cylinder acts as a divider within the fluid domain and not as a separate body or firm boundary.

B. Mesh

Initially the mesh that was created for this domain was limited by the 512,000 cell limit that we had on certain computers. This proved to be an insufficient number of cells for our analysis.

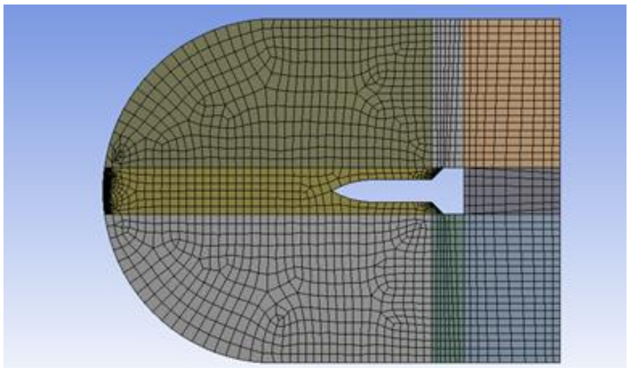

Figure 16: Structured but coarse missile mesh

Even after using an inflation layer to create a relatively refined mesh region around the surface of the missile, most flow characteristics (development of a boundary layer, shockwave formation, the formation of vortices downstream of the rocket) remained undefined.

However, once we were granted access to computers with higher levels of Fluent licensing it became possible to further refine the mesh. At the outset this was tried with edge sizing techniques similar to those found in Cornell airfoil analysis tutorials [6}. This proved to be an involved task with our more complicated geometry and this strategy was abandoned in favor of a larger inflation layer around the rocket body and a controlled inflation rate and maximum cell size for the mesh as a whole.

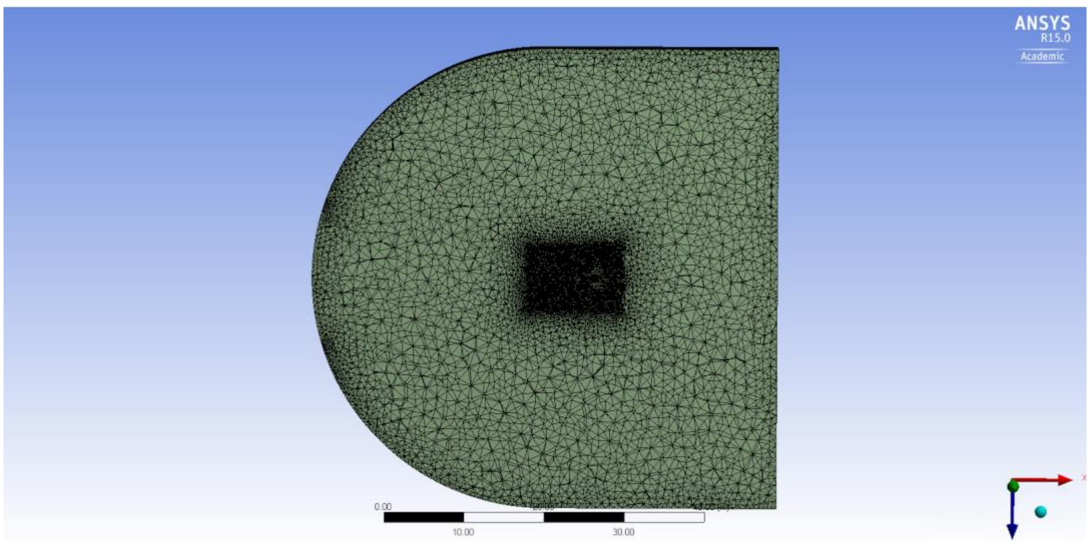

Figure 17: 3D Missile Mesh used for Analysis

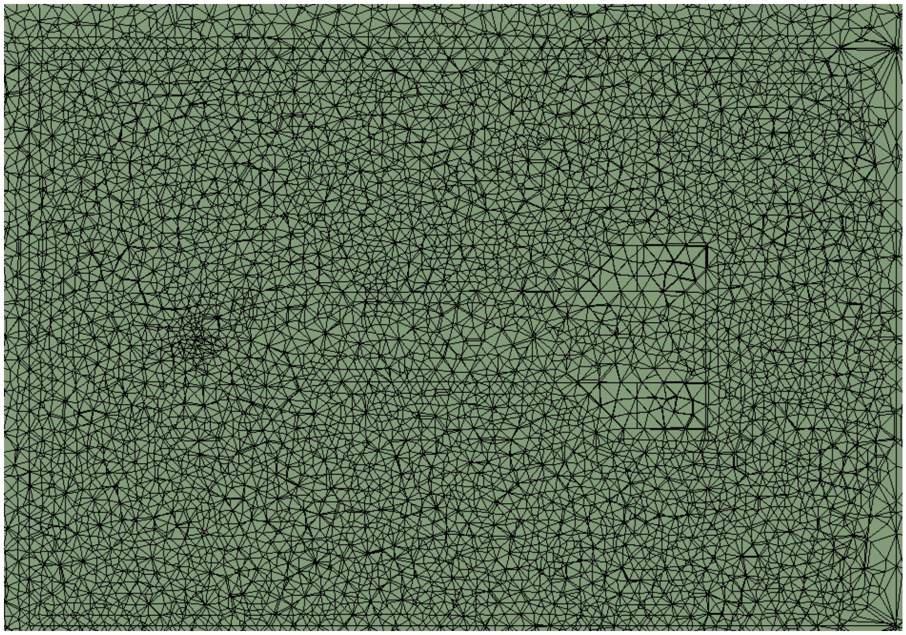

Figure 18: Closer View of 3D Missile Mesh

Even with these conditions it seemed that flow features were not fully developed so a cylinder was added to divide the geometry as described above. A body of influence centered around the nose of the missile and applying to the smaller cylindrical body was created and a smaller mesh condition with a mesh element size of .2m was applied as opposed to .8m throughout the rest of the fluid domain. Growth rate for the inflation of the fluid domain outside the cylindrical refinement was allowed to be the standard value of 1.2. The generated a mesh of 1,510,894 cells which we imported into Fluent solver.

C. Setup

The materials considered were an aluminum body for the missile and air considered as a compressible ideal gas for the fluid domain. The aluminum body was, of course, considered to be a solid wall. In some previous simulations, the inlet (or semicircular surface) was considered to be a velocity inlet and the sides and walls were set as pressure-outlets. For this case we set the inlet and both the side and back end outlet regions as far field pressure outlets. This allowed us to define a common Mach number of 1.2 for all of them simulating the flight of a vehicle in relatively unbounded space.

D. Solution

While not all the equations converged to the desired residual power 10^-3, the simulation images below show the flow characteristics that we expected to be displayed, making it a viable basis for jet analysis.

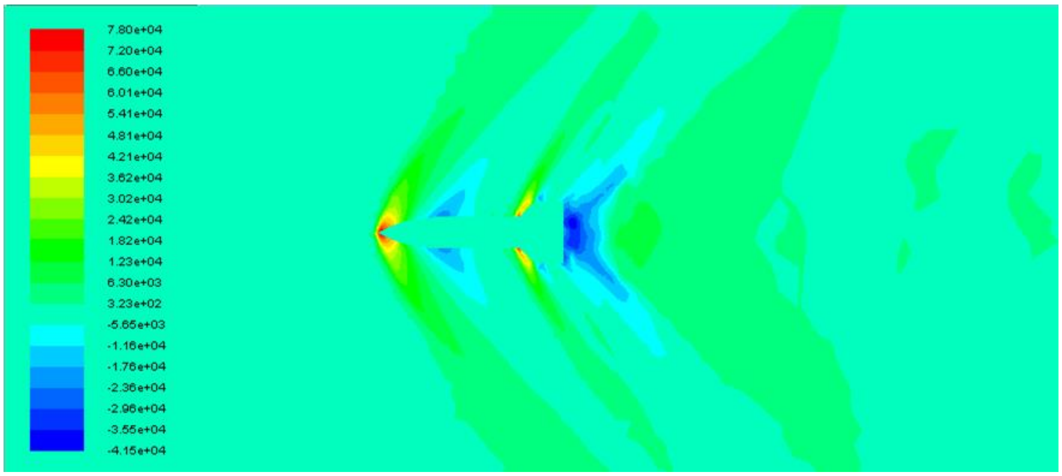

Figure 19: 3D Finned Missile, Contours of Pressure

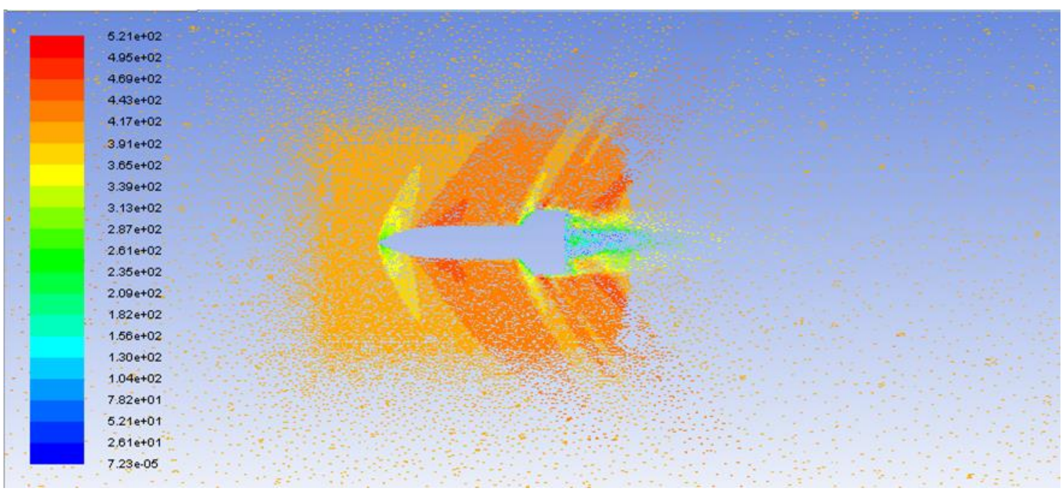

Figure 20: 3D Finned Missile, Velocity Vectors

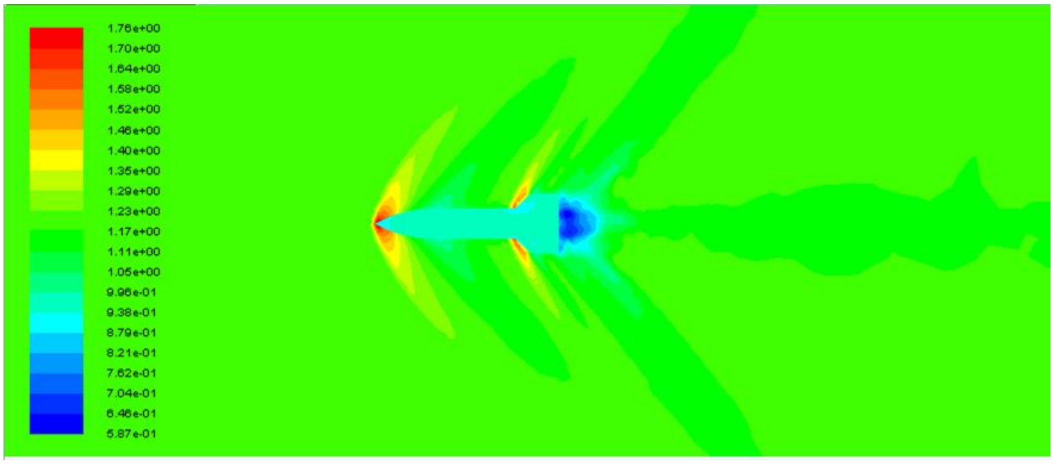

Figure 21: 3D Finned Missile, Contours of Density

IV. 3-Dimensional Missile Geometry with Jet

After a successful meshing and solution of the missile geometry we proceeded to add a jet to the missile surface. There is an unresolved issue defining this as a velocity inlet. The missile geometry and mesh are shown below.

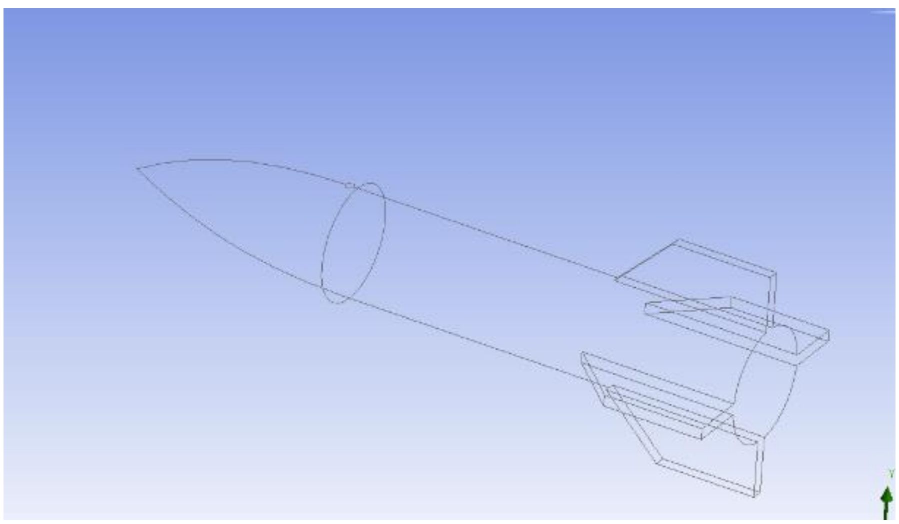

Figure 22 Missile with Jet Geometry

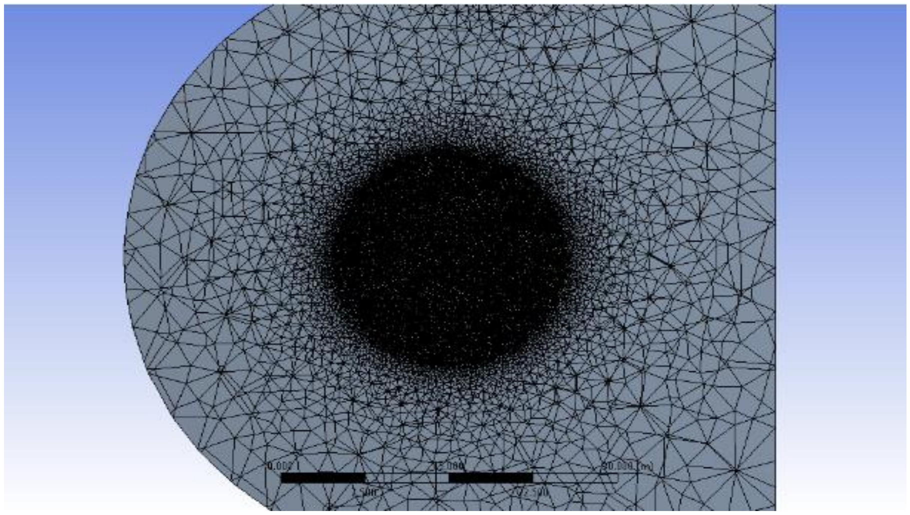

Figure 23 Meshing for Missile with Jet

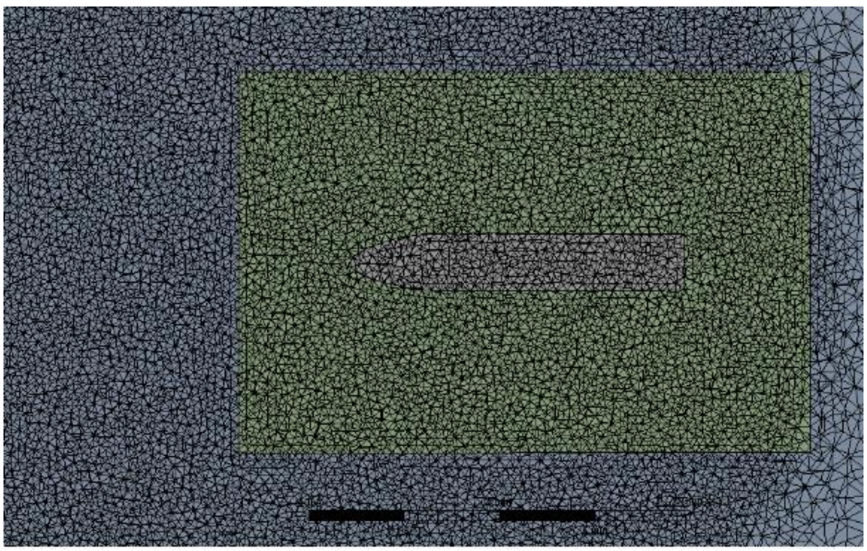

Figure 24 Closer view of Meshing for Missile with Jet

Conclusion

With the help of our faculty advisor and his previous graduate student we were able to reproduce past experimental analysis. Starting with the 2-dimensional analysis we recreated the flat plate geometry all together with a shorter top wall and got similar results as previous testing. With these results we were ready to be able to take the next step and move to 3-Dimensional analysis. Having the help of the graduate student we were able to recreate the 3-Dimensional flat plate similar to his initially with only a shorter downstream section for the lack of element size. Even with the shorter domain and smaller cell size were able to see good pressure distributions and the start of shock waves. Once we were able to have a larger element capacity it help greatly with the ability to have the solution converge. With the converged results we were able to see a tremendously more detailed solution.

The application of the project was to see some of the pressure distributions on the flat plate only on a 3-dimensional air vehicle. In the analysis of the 3-dimensional rocket body that had a geometry closely recreated by the J. Brandeis and J. Gill experiment we had only the missile body with no jet. From there we saw a solid pressure distribution along the body of the missile as well as shock waves that were expected to be seen.

References

[1] Povitsky and K. Pierson, Transient Effects of Sonic Control Jet Configurations Acting in a Supersonic Crossflow, Control ID: 2649344, submitted to the 2017 AIAA Aviation and Aeronautics Forum and Exposition conference.

[2] J. Brandeis and J. Gill, “Experimental Investigation of Super- and Hypersonic Jet Interaction on Missile Configurations,” Journal of Spacecraft and Rockets, vol. 35, no. 3, pp. 296–302, 1998

[3] J. Santiago and J. Dutton, "Velocity Measurements of a Jet Injected into Supersonic Crossflow," Journal of Propulsion and Power, vol. 13, no. 2, pp. 264-273, 1997.

[4] *Screen clippings from Ansys FLUENT*

[5] Walker-Horn, Ariane Veronica. "3D Transonic Flow Over a Wing - Pre-Analysis & Start-up." Dashboard. Cornell University, 06 July 2015. Web. 28 Apr. 2017.

[6] "Flow Over an Airfoil." Dashboard. Cornell, n.d. Web. 10 May 2017.